SYNTHESIS AND ANALYSIS OF Al-BASED NANOPOWDERS

C. Mihoc[1,2], E. Burkel[1]

[1]Institute of Physics, University of Rostock, August-Bebel-Str. 55, D – 18055 Rostock, Germany
[2]Faculty of Food Enginnering, Stefan cel Mare University of Suceava, Universitatii 13, 720225 Suceava, Romania

Abstract: *In this paper the synthesis and phase formation of high-energy ball-milled Al-Cu-Fe alloy powders has been studied. The chemical homogeneity and microstructure of the powders were investigated using scanning electron microscopy (SEM/EDX). The sequences of solid-state phase transformation were examined by in situ high-temperature synchrotron radiation diffraction (HTXRD) at HASYLAB/DESY.*

Keywords: Quasicrystals; Al-based alloys; Powder metallurgy; Mechanical alloying

Introduction

Since the discovery of icosahedral phases in rapidly-quenched Al-Mn alloys [Sh'84], quasicrystals (QCs) were observed in over 100 alloy systems. Among them, the ternary Al–Cu–Fe alloy is most interesting [Sa'01, Sr'00, Tr'03], thanks to excellent properties, such as the low electrical and thermal conductivity, high hardness, low friction and wear, and good oxidation resistance. The synthesis of single-phase Al–Cu–Fe QC's by conventional casting is difficult, due to their very narrow composition domain [Lü'03]. Recent research efforts were devoted to the mechanosynthesis of quasicrystalline Al–Cu–Fe powders by powder metallurgy (P/M) routes [Mu'04, Ni'07, Sc'03, Tc'02, Yo'05]. The main aim of the present work is to investigate the formation of icosahedral (iQC) phases.

Experimental

Nanocrystalline (nc-) Al–Cu–Fe powders were prepared by mechanical alloying (MA) in a planetary ball mill (RETSCH PM400). Wet-milling in hexane was employed to counteract severe powder losses during MA [Fl'01, Sc'03], avoid severe contamination from grinding media and prevent oxidation effects. No other milling additives were used. High purity powders of Al (99.95%), Cu (99.95%) and Fe (99.95%) were loaded into 250 ml hardened chromium–steel vials together with 10 and 20 mm steel balls. The ball-to-powder ratio (BPR) was chosen approximately equal to ≈14:1. The resulting Al-Cu-Fe powders were dried at room temperature, then shaped into disk pellets (Φ 5mm) by uniaxial pressing (200kN) and sintered in vacuum during 1h at 800^{0}C.

During high-energy ball-milling, the initial shape of the starting powder particles is lost and the powders are flattened by severe plastic deformation processing. Subsequent cold welding leads to the formation of solid-solution/alloy phases as lamellar aggregates. These aggregates will further undergo fragmenting. The competing cold welding and fragmentation balance towards an equilibrium morphology for long ball-milling times. Beyond a certain milling time no further refinement of the

microstructure occurs and the equilibrium morphology is usually given by a bimodal particle-size distribution.

The formation of QC's during non-isothermal annealing of the Al–Cu–Fe nanopowders was studied by high temperature synchrotron radiation diffraction (HTXRD). The in-situ X-ray diffraction experiments were performed at the MAX 80 installed at the F2.1 beamline of HASYLAB/DESY in Hamburg, Germany (fig.1). The MAX80 instrument uses a cubic-anvil-type press, which is known to provide better results for isotropic pressure generation compared to other multiple-anvil high-pressure devices [He'02]. The external pressure is generated by six syncronized anvils (sintered 6Co-WC). Teflon sheets are squeezed between the anvils, in order to reduce friction and provide electrical insulation during high-temperature experiments.

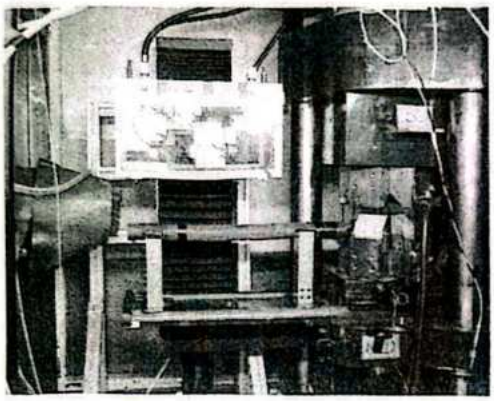

Figure 1 General view of the high-pressure MAX80 setup at the F2.1 beamline at HASYLAB.

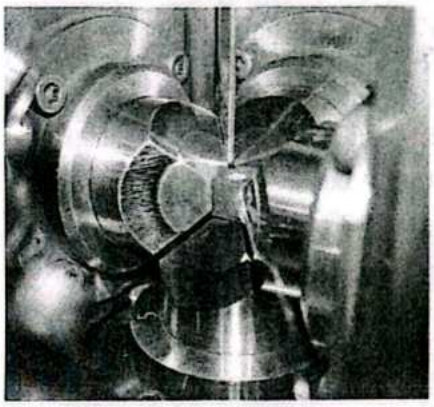

Figure 2 Geometric arrangement of the WC anvils and the amorphous boron cube (sample container).

The applied force is generated by an uniaxial hydraulic press, and equally transmitted to each of the faces of the cubic pressure medium formed by the anvils (Fig. 2). White (energy-dispersive EDX mode) incident X-rays beam was used.

The energy dispersive X-ray diffraction (EDX) method was first reported by Buras et al. in 1968 [Bu'68] and is primarily used to determine the crystallografic structure of polycrystalline powders.

The EDX method relies on the use of a well-collimated and polychromatic (white) incident synchrotron radiation beam [St'81, Sk'83].

The photon energy distribution of diffracted photons, measured at a fixed scattering angle ($2\theta_0$), has the role of an analyser. Each {hkl} set of crystal lattice planes with interplanar spacing d_{hkl} will select from the incident white beam and scatter into the detector only those photons having an energy E_{hkl} satisfying the Bragg equation :

$$2d_{hkl}\sin\theta_0 = \lambda_{hkl} = \frac{hc}{E_{hkl}} = \frac{12.398}{E_{hkl}} \quad (\text{keV}\cdot\text{Å}) \qquad (1)$$

where λ is given in Å and the energy in keV (h is Planck's constant and c the velocity of light). The Bragg equation is usually written in the more convenient form :

$$d_{hkl}E_{hkl}\sin\theta_0 = 6.199 = C \qquad (2)$$

where the constant term C is given in (keV·Å). The integrated intensity of a reflection record by the detector along a unit length of the Debye-Scherrer ring is given by the formula [Bu'89]:

$$I_{hkl}(E) = C \cdot \left\{ I_0(E) \cdot E^{-2} \cdot m|F|^2 \cdot \eta(E) A(E,\theta_0) \cdot L_p(E,\theta_0) \right\}_{hkl} \cdot \sin^{-3}\theta_0 \cdot \Delta\theta_0 \qquad (3)$$

where C is a constant for a given experiment (given by Eq. 2), $I_0(E)$ is the incident beam intensity per unit energy range, m_{hkl} the multiplicity factor, and F_{hkl} the structure factor including the atomic scattering factors with the corresponding Debye-Waller factor and $\Delta\theta_0$ is a convolution of the incident and diffracted beam divergences. $\eta(E)$ is the detector quantum efficiency, which must either be measured or taken from efficiency curves supplied by the detector producer. $A(E,\theta_0)$ is the attenuation (absorption) factor and $L_p(E,\theta_0)$ the polarization factor. The high-pressure set-up used at F2.1 beamline (HASYLAB) has a vertical scattering plane, which has the advantage that $L_p(E,\theta_0) \approx 1$ for all energies and all scattering angles.

The powder sample is mounted inside a amorphous boron - epoxy resin cubic container of either 4 or 6 mm edge size (Fig. 3). A graphite cylinder and copper rings are provided for current heating. The specimen is mounted within a boron nitride cylinder together with the pressure calibration material (NaCl). Boron nitride powder layers further separate the sample from the NaCl pressure marker and the graphite cylinder, so that the sample is protected against chemical contamination during the diffraction experiment.

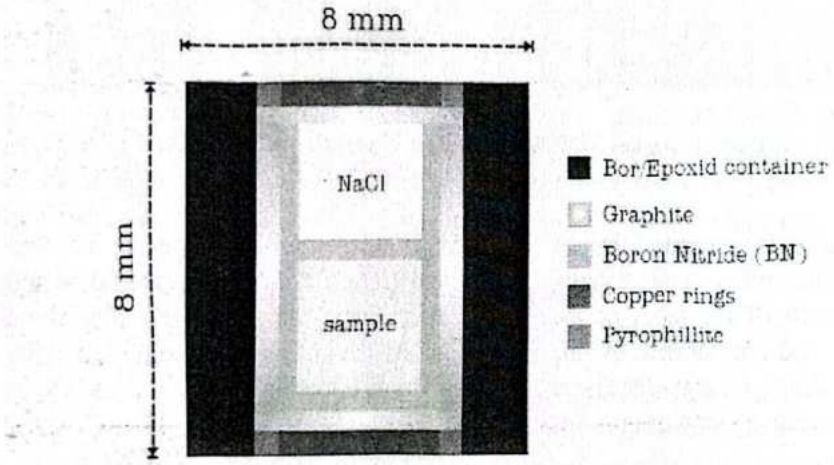

Figure 3 Schematic illustration of the high-pressure sample preparation procedure.

The XRD patterns were collected each 10 ◦C during constant heating.

SEM images of the obtained powders have been coupled with energy dispersive X-ray (EDX) and chemical mapping on a few micron-sized window.

Results and Discussion

Al–Cu–Fe alloy nanopowders with particle sizes between 10 and 20 μm were obtained after wet-milling in hexane for 25 h at 200 rotations per minute. SEM micrograph of the as-milled powders indicates a fairly uniform, ultrafine microstructure of the alloy. Neither large pore agglomerates or exaggerated grain-growth are noticed (Fig. 4). The chemical composition of the as-milled powders equals $Al_{65}Cu_{15}Fe_{10}$ as shown by energy dispersive X-ray EDX in Fig. 5. The sintered specimens still exhibit uniform

porosity in the submicron range. Chemical mapping by SEM/EDX further confirmed the high homogeneity of the sintered pellets (Figure 6).

Rapid densification is achieved without alteration of the initial ultrafine microstructure of the starting powders.

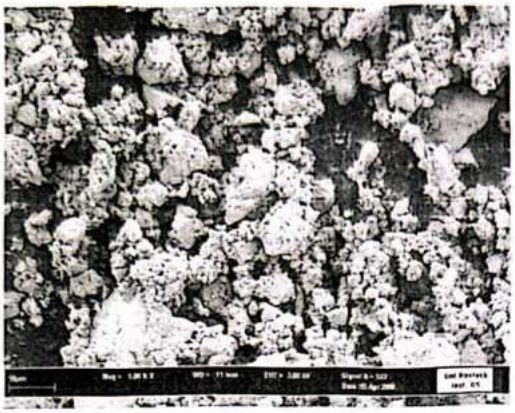

Figure 4 SEM micrograph of the as-milled Al-Cu-Fe alloy

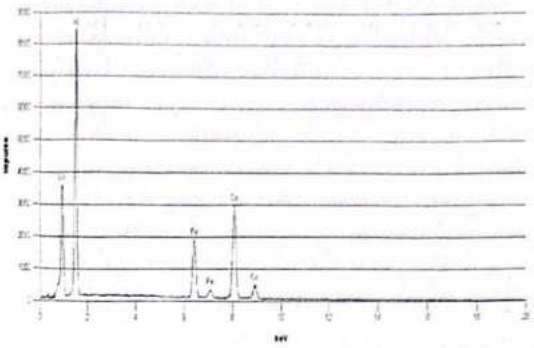

Figure 5 EDX spectra of the Al-Cu-Fe alloy

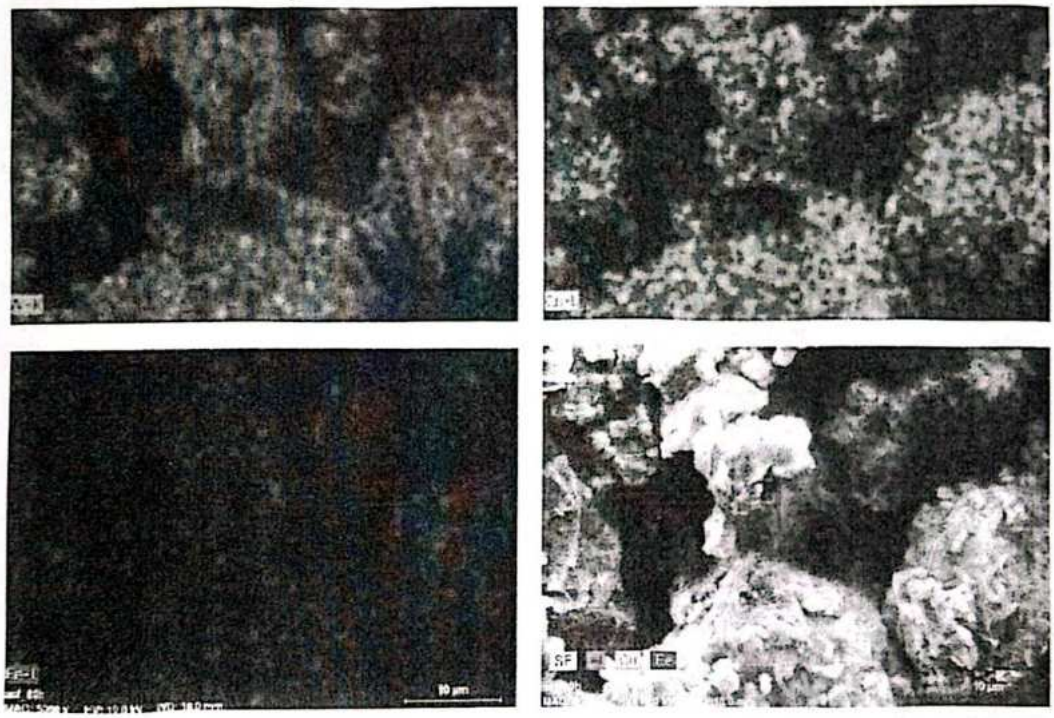

Figure 6 EDX composition maps, showing the spatial distribution of Al, Cu and Fe.

The high-temperature HTXRD patterns of the Al-Cu-Fe powders during constant-rate heating at 10 ◦C/min. are shown in Fig. 7. The phase constitution of the Al-Cu-Fe alloy changes several times upon heating: the *in situ* synchrotron radiation diffraction experiment reveals a significant overlapping of the thermal stability fields of the constituent alloy phases.

The selected diffraction pattern at 800^{0}C is also shown (Fig. 8), to illustrate in

more detail the formation of a single icosahedral phase between 750 – 800°C, in good agreement with other literature results. At lower temperatures, Al_2Cu and Fe_3Al phases are present, mainly due to the positive heat of mixing (15 kJ/mol) of the Fe–Cu pair.

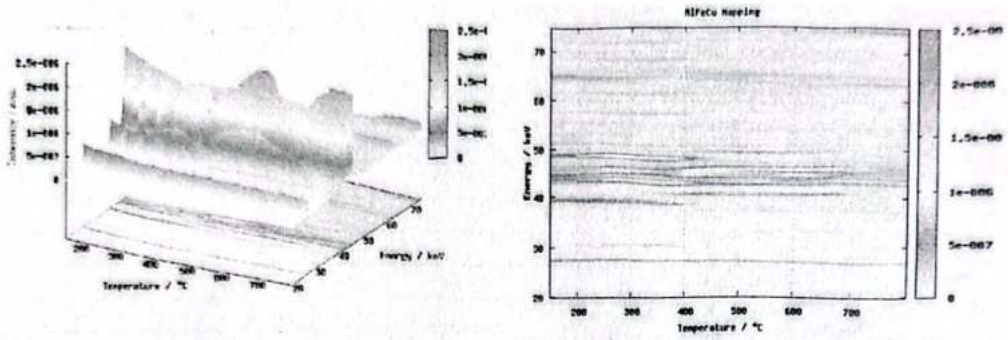

Figure 7 *In situ* high-temperature diffraction(HTXRD) patterns of Al–Cu–Fe alloy powders showing the phase evolution towards the formation of single-phase quasicrystals above 750°C.

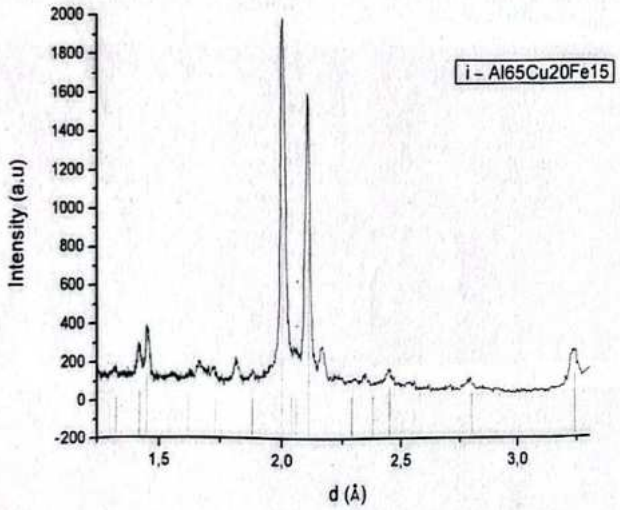

Figure 8 Selected XRD pattern collected at 800°C showing the icosahedral-Al65Cu20Fe15 single phase.

The ω-Al_7Cu_2Fe phase is the main precursor of the i-$Al_{65}Cu_{20}Fe_{15}$ phase. As the homogenisation of the alloy composition is gradually completed, the ω-Al7Cu2Fe becomes the major constituent phase. Minor traces of Fe_3Al were still noticed in the XRD patterns after the nucleation of the iQC phase at approximately 600°C.

Conclusions

Nanocrystalline powders were obtained by ball-milling of pure elemental powders in liquid media. Single-phase quasicrystalline powders result from subsequent non-isothermal annealing above 750°C. The wet-milling route prevents oxidation, powder losses or contamination from the grinding media. The mechanical alloying process followed by non-isothermal thermal treatment at constant heating rate are effective in providing single-phase icosahedral quasicrystalline powders.

Pressing and vacuum sintering results in homogeneous bulk solids with uniform ultrafine microstructure. Research is underway to investigate the properties of the quasicrystals, like mechanical response, as well as the wear and oxidation resistance.

Acknowledgements

This work was supported by the European Marie Curie Programme through ADVATEC project (EU Marie Curie EST, 2005-2009, Contract No. MEST-CT-2005-020986).

References

[Bu'68] B. Buras, J. Chwaszczewska, Z. Szmid, Inst. Nucl. Res. Warsaw, Rep. No. 894/II/PS, 1968.

[Bu'89] B. Buras, L. Gerward, Application of X-ray energy-dispersive diffraction for characterization of materials under high-pressure, Prog. Crystal Growth and Charact. 18, 1989, 93-138.

[Fl'01] E. Fleury, J.H. Lee, S.H. Kim, G.S. Song, J.S. Kim, W.T. Kim, D.H. Kim, Mater. Res. Soc. MRS 643, 2001, K2.1.1–K2.1.6.

[He'02] R.J. Hemley, G.L. Chiarotti (eds.), High pressure phenomena, IOS Press, Amsterdam, 2002.

[Lü'03] R.Lück, L.Zhang, in Ref. [2],2003,26–44.

[Mu'04] B.S. Murty, P. Barua, V. Srinivas, J. Eckert, J. Non-Cryst. Solids 334–335,2004, 44–47.

[Ni'07] R. Nicula et al., J. Alloys Compd. 434-435, 2007, 319-323.

[Sa'01] A.I. Salimon et al, Acta Mater. 49, 2001, 1821.

[Sc'03] F. Schurack, J. Eckert, L. Schulz, in: H.-R. Trebin (Ed.), Quasicrystals, Wiley-VCH, Weinheim, 2003, pp. 551–569.

[Sh'84] D. Shechtmann, I. Blech, D. Gratias, J.W. Cahn, Phys. Rev. Lett. 53 (1984) 1951.

[Sk'83]. E.F. Skelton, S.B. Quadri, A.W. Webb, C.W. Lee, J.P. Kirkland, Rev. Sci. Instrum. 54, 1983, 403.

[Sr'00] V. Srinivas, P. Barua, B.S. Murty, Mater. Sci. Eng. 294-296, 2000, 65-67.

[St'81] J. Staun Olsen, B. Buras, L. Gerward, S. Steenstrup, J. Phys. E. 14, 1981, 1154.

[Tc'02] V.V. Tcherdyntsev, S.D. Kaloshkin, A.I. Salimon, E.A. Leonova, I.A. Tomilin, J. Eckert, F. Schurack, V.D. Rogozin, S.P. Pisarev, Yu.P. Trykov, Mater. Manufact. Proc. 17, 2002, 825–841.

[Tr'03] H-R. Trebin (Ed.), Quasicrystals, Wiley-VCH, Weinheim, 2003.

[Yo'05] X. Yong, I.T. Chang, I.P. Jones, J. Alloys Compd. 387, 2005, 128–133.